Title: Ear wound healing in MRL/MpJ mice is associated with gut microbiome composition and is transferable to non-healer mice via microbiome transplantation

Author Block:

Cassandra Velasco[2]

Christopher Dunn[2]

Cassandra Sturdy[1]

Vladislav Izda[1]

Jake Martin[1]

Alexander Rivas[3]

Jeffrey McNaughton[2]

Matlock A. Jeffries[1,2] (ORCID ID: 0000-0001-9516-4312)

1. Oklahoma Medical Research Foundation, Arthritis & Clinical Immunology Program, Oklahoma City, OK
2. University of Oklahoma Health Sciences Center, Department of Internal Medicine, Division of Rheumatology, Immunology, and Allergy, Oklahoma City, OK
3. University of Arkansas for Medical Sciences, Little Rock, AR

Contact information for correspondence:

Matlock A. Jeffries, MD

Oklahoma Medical Research Foundation

825 NE 13th Street, Laboratory MC400

Oklahoma City, OK 73104

Phone: (405) 271-7438

Fax: (888) 319-1241

Email: matlock-jeffries@omrf.org

Acknowledgments and Affiliations:

This work was supported by NIH grants K08AR070891, P20GM125528, R61AR078075, and R01AR076440, along with the Congressionally Directed Medical Research Program grant PR191652. The content is solely the responsibility of the authors and does not necessarily represent the official views of the National Institutes of Health. The funding source had no involvement in the writing of this article.

This work was supported by a Physician Scientist Development Award (PDSA) from the Presbyterian Health Foundation and an Oklahoma Center for the Advancement of Science and Technology (OCAST) Oklahoma Health Research Grant.

COI: The authors declare no conflicts of interest.

Abstract:

Objective: Adult cartilage has limited repair capacity. MRL/MpJ mice, by contrast, are capable of spontaneously healing ear punctures. This study was undertaken to characterize microbiome differences between healer and nonhealer mice and to evaluate microbiome transplantation as a novel regenerative therapy.

Methods: We transplanted C57BL/6J mice with MRL/MpJ cecal contents in mice at weaning and as adults (n=57) and measured earhole closure 4 weeks after a 2.0mm punch and compared to vehicle-transplanted MRL and B6 (n=25) and B6-transplanted MRL (n=20) mice. Sex effects, timing of transplant relative to earpunch, and transgenerational heritability were evaluated. In a subset (n=58), cecal microbiomes were profiled by 16S sequencing and compared to earhole closure rates. Microbial metagenomes were imputed using PICRUSt.

Results: Transplantation of B6 mice with MRL microbiota, either in weanlings or adults, improved earhole closure rates. Transplantation prior to ear punch was associated with the greatest earhole closure. Offspring of transplanted mice healed better than controls. Several microbiome clades were correlated with healing, including Firmicutes, Lactobacillales, and Verrucomicrobia. Gram-negative organisms were reduced. Females of all groups tended to heal better than males, female microbiota resembled MRL mice.

Conclusion: In this study, we found an association between the microbiome and tissue regeneration in MRL mice and demonstrate that this trait can be transferred to nonhealer mice via microbiome transplantation. We identified several microbiome

clades associated with healing. Future studies should evaluate the mechanisms underlying these findings and confirm our results in murine OA.

Introduction

The Murphy Roths Large (MRL) mouse strain was originally selected for large body size in the 1960s; at the F_{12} generation, these mice developed a spontaneous mutation in the immune regulator *Fas*. This MRL/*lpr* variant is commonly used as a lupus mouse model [1,2], whereas the non-*Fas*-mutant MRL/MpJ strain are generally used as a control in autoimmune disease experiments. In 1998, MRL/MpJ mice were unexpectedly found to fully close 2.0mm earhole puncture wounds after 4 weeks [3,4], subsequent studies have shown a generalized healing phenotype in MRL mice, including neonatal digital tip regrowth [5,6], peripheral nerve regeneration [7], and cardiac wound healing [8,9].

Approximately 75% of the MRL genome is derived from the LG/J parent strain. In experiments over the past decade, several backcrosses of LG/J and SM/J (a nonhealer strain) have been generated to evaluate the heritability of earhole closure and OA protection. Those backcrosses most genetically similar to LG/J mice have the greatest regenerative earhole wound healing capacity [10], as well as the highest articular cartilage regeneration ability [11,12]. Genetic analyses of these strains have been conducted [13–16], with several genes and gene pathways now known to be involved with wound healing [17], including DNA repair and Wnt signaling [16]. However, a 2015 report made an unexpected discovery: C57BL/6J mice did not improve either ear-wound or articular cartilage healing following an allogeneic bone marrow transplant from MRL/MpJ donors [18], and a recent study found the heritability of OA protection in

LG/SM backcrosses to be only moderate (0.18 to 0.58) [19], suggesting that other environmental factors play a role in MRL healing.

Of particular human relevance, MRL mice also regenerate knee cartilage following full-thickness cartilage injury [20], protecting them against the development of osteoarthritis (OA) Further studies have demonstrated a strong correlation between this articular cartilage healing phenotype and healing of ear puncture holes [11]. OA is a chronic musculoskeletal disease characterized by pain and progressive loss of joint function leading to reduced mobility and is associated with a variety of comorbidities including heart disease, stroke, metabolic syndrome, and anxiety/depression [21–23]. It is the most common musculoskeletal disease worldwide and is the leading cause of chronic disability in the US, affecting roughly half of adults over 65 years of age [24]. There are no disease modifying drugs approved for OA; therefore, much attention has recently been focused on the development of novel regenerative strategies to treat this devastating disease.

In the present study, we set out to investigate whether the gut microbiome is associated with the cartilage healing phenotype observed in MRL mice generally, whether this trait is transferable to nonhealer mice via alteration of the gut microbiome, and whether microbiome differences are associated with sex-associated discordant ear hole closure rates in MRL mice.

Methods

Ethics Statement:

The institutional review board and institutional animal care and use committees of all involved institutions approved this study; a detailed protocol was developed prior to beginning this study; this protocol and subsequent addenda were reviewed by the animal care and use committee of all involved institutions.

Mouse husbandry:

Young male and female (4 week-old) C57BL6/J or MRL/MpJ mice were purchased from Jackson Laboratories (Bar Harbor, ME, USA) and housed at the Oklahoma Medical Research Foundation (OMRF). Breeding pairs were created and pups were used for some experiments. All animals were permitted ad libitum access to food and water (NIH31). The OMRF animal facility uses a 12-hour light-dark cycle. All animal husbandry procedures adhered to the NIH Guide for the Care and Use of Laboratory Animals. There were no adverse events (expected or unexpected) during the course of this experiment.

Mouse cecal microbiota transplantation procedure:

Cecal donor mice (B6 or MRL, 10-14 weeks of age) were sacrificed and immediately dissected under sterile conditions. The cecum was removed and cecal contents transferred to a sterile tube containing a 1:1 mixture of glycerol and phosphate-buffered saline (5mL), which was then filtered through a 100μM filter. The resulting mixture was aliquoted and frozen at -80C for subsequent transplantation. At 3-4 weeks of age,

recipient mice were pretreated with omeprazole (50mg/kg body weight) as previously described [25,26]. Omeprazole was then sequentially administered via oral gavage once daily for 3 days prior to microbiome transfer. On the day of cecal transplantation, 100uL of transplant material (per 3-4-week-old recipient mouse) or 300uL of transplant material (per 16-week-old adult mouse) was transplanted via oral gavage using flexible 30mm polypropylene tubes (Instech, Plymouth Meeting, PA, USA). Mice were then moved to clean cages and segregated by transplant group. For adult transplantation experiments, 12 week-old mice were given 50mg/kg omeprazole once daily for 3 days, then transplanted on day 4, as above.

Mouse earhole puncture, sacrifice procedures:

At 6 weeks of age (for young animals) or 18 weeks of age (for adult animals), mice were ear punched using a 2mm through-and-through ear punch. Mice were sacrificed 4 weeks after ear punch (10 weeks of age for young and 22 weeks of age for adult animals). Whole blood was collected via cardiac puncture, allowed to clot for at least 30 minutes, then centrifuged and serum removed for subsequent analysis. Final earhole size was measured using digital calipers, investigators were blinded to mouse group during earhole size measurements. Cecal material was collected immediately after sacrificing animals and flash frozen in liquid nitrogen. Cecal DNA was extracted using a QIAamp DNA microbiome kit (Qiagen).

16S ribosomal RNA (rRNA) gene sequencing:

Microbial profiles were determined by sequencing a ~460bp region including the V3 and V4 variable region of bacterial 16S rRNA genes. The gene fragment was amplified from approximately 30ng of DNA in each sample (primers in Supplementary Table 1) using a high-fidelity polymerase (NEB Q5, New England Biolabs)[27] and confirmed by 1% agarose gel electrophoresis. PCR master mixes were decontaminated with double-stranded DNAse treatment (PCR decontamination kit, Arcticzymes, Tromsø, Norway). Sterile water was processed using the same procedure as a negative control. Illumina Nextera XT indices were attached (Illumina), pooled in equimolar amounts, and sequenced on an Illumina miSeq sequencer using a 300bp paired-end sequencing protocol by the Clinical Genomics Center at OMRF.

16S rRNA OTU classification:

Quality filtering, operational taxonomic unit (OTU) classification and microbial diversity analysis were performed using the Quantitative Insights into Microbial Ecology (QIIME) software package, version 1.9.1[28]. Sequences were assigned to OTUs using the UCLUST algorithm[29] with a 97% pairwise identity threshold and taxonomy assigned using the GreenGenes 13_8 database[30].

Diversity analyses:

Alpha diversity was characterized using the observed OTUs method following rarefaction to the lowest number of OTUs present per group (123,543). Beta diversity was evaluated on a variance-adjusted, weighted unifrac model. Principal component analysis was performed and an Adonis (permuted analysis of variance, a multi-factor

PERMANOVA) test with 999 permutations was used to calculate the statistical significance of group differences[31,32].

Group analyses:

Group analyses were performed using the linear discriminant analysis effect size (LEfSe) pipeline[33]. LEfSe performs a non-parametric Kruskal-Wallis sum-rank test[34] to detect features with significant differential abundance between groups, $P \leq 0.01$ was considered significant. Next, it uses a linear discriminant analysis (LDA)[35] to estimate the effect size of each differentially abundant feature. An LDA threshold of ≥2 was considered significant[36]. QIIME was used to calculate group Benjamini-Hochberg FDR-corrected q-values; $q \leq 0.01$ was chosen as the 'FDR-corrected' significance threshold. For Gram status comparisons, differences were evaluated by Student t-tests, $P \leq 0.05$ was considered statistically significant. Correlations were determined by comparing earhole closure rates of individual animals with microbiome clades, $P \leq 0.05$ was considered statistically significant. No samples were excluded from analysis.

Prediction of metagenome content and imputed bacterial functional classification:

The Phylogenetic Investigation of Communities by Reconstruction of Unobserved States (PICRUSt) software package[37] was used to impute bacterial metagenomes from our 16S deep sequencing microbial DNA data, and functional annotation applied using the Kyoto Encyclopedia of Gene and Genomes (KEGG) catalog[38]. Statistical analysis was performed using the Statistical Analysis of Metagenomic Profiles (STAMP) package[39]. Statistical significance and effect sizes among the three groups (human

OA-eroded, OA-intact, and control) were calculated using ANOVA. Statistical significance was defined as Benjamini-Hochberg FDR corrected $P \leq 0.01$.

Results:

Improved earhole closure in non-healer B6 mice transplanted with healer MRL cecal material

Our final analysis included 131 mice from 6 independent experiments. These included 25 B6 vehicle-transplanted control mice, 57 MRL-transplanted B6 mice, 29 MRL vehicle-transplanted control mice, and 20 B6-transplanted MRL mice. B6-vehicle mice healed earhole punches poorly (0.25±0.03mm, earhole healing 4 weeks after a 2mm earhole punch, mean±SEM), whereas MRL-vehicle mice healed well (1.4±0.1mm). MRL-transplanted B6 mice healed roughly three times as well as B6-vehicle mice, and half as well as MRL-vehicle mice (0.74±0.05mm, P=6.9E-10 vs. B6-vehicle, P=5.2E-12 vs. MRL-vehicle, **Figure 1A**). Transplantation of MRL mice with B6 cecal material did not reduce MRL healing (B6-transplanted MRL 1.3±0.1 vs. MRL-vehicle 1.4±0.1, p=0.36).

Earhole closure outcomes depend on the timing of microbiome transplantation

Next, we determined whether the timing of microbiome transplantation relative to ear punch would alter this healing phenotype. We performed ear punches of 6 week-old male B6 mice, similar to previous experiments, then performed an MRL cecal transplantation at 48 hours, 1 week, and 2 weeks after ear punch. There was a graded

reduction in ear wound healing capacity in mice transplanted after ear punch (**Figure 1B)**; the 48 hour post-ear punch group (n=8) demonstrated superior healing compared to B6-vehicle mice (0.56±0.06mm vs. 0.25±0.03mm, P=2.4E-5, n=8), although there was a trend towards worse healing than mice transplanted at weaning (P=0.11). In mice transplanted 1 week after ear punch, there was a trend towards improved healing (0.35±0.05mm, P=0.11, n=7). Healing was not improved compared to vehicle controls in mice transplanted 2 weeks after ear punch (0.26±0.05mm, P=0.93, n=6).

Adult transplant recipients heal as well as weanling recipients

Although previous studies have indicated that the gut microbiome is most plastic in mice at weaning [40], the disease our laboratory studies (OA) is a disease of adulthood. Therefore, to broaden the applicability of our findings, we evaluated whether transplantation of mice as adults would still confer improvements in earhole closure. To this end, we performed cecal transplantation of B6 mice with MRL donor material (n=7) or vehicle (n=4), as previously described, in 12 week-old mice with earhole punch 3 days later. No differences in earhole closure rate were seen in mice transplanted at weaning compared to mice transplanted as adults (**Figure 1C**) (B6-vehicle weaning: 0.25±0.03mm earhole closure vs. adult: 0.25±0.07, *P*=0.47; MRL-transplanted B6 weaning: 0.74±0.05 vs. 0.60±0.06, *P*=0.25).

Disparate healing rates in mice raised in-house compared to mice sourced from a commercial vendor

Both the bacterial and viral components of the mouse gut microbiome are heavily influenced by diet and other environmental factors; in fact, previous studies have noted dramatic differences in the microbiome when comparing the same strain of mouse obtained from different commercial vendors [41,42]. Roughly half of our mouse experiments were conducted on mice raised in-house (originally from Jackson laboratories, but bred for use at OMRF, including donors and recipient animals), with the other half being purchased commercially from Jackson laboratories and immediately used for transplantation experiments as both donors and recipients. We found variations earhole closure rates with in-house reared mice demonstrating worse healing in the B6-vehicle group (commercial vendor: 0.31±0.03mm earhole closure vs. in-house: 0.16±0.05, P=0.01) and improved healing in MRL-transplanted B6 (vendor: 0.57±0.04 vs. 0.86±0.07, P=0.0036), with a trend towards improved healing in MRL-vehicle mice (vendor: 1.38±0.06 vs. 1.65±0.1, P=0.08) (**Figure 1D**).

Transgenerational heritability of microbiome-mediated improvements in earhole closure

We then evaluated the heritability of improved earhole closure following microbiome transplantation. We transplanted mice at weaning, as previously discussed, then created breeding pairs consisting of MRL-transplanted B6 male with MRL-transplanted B6 female, B6-vehicle male with MRL-transplanted B6 female, and MRL-transplanted B6 male with B6-vehicle female. The offspring of these breeding pairs were ear punched at 6 weeks of age and earholes measured 4 weeks later to align with the timeline of our previous transplantation-at-weaning experiments. We found offspring of transplanted mice healed significantly better than non-transplanted control mice

(0.63±0.03mm, mean±SEM vs. 0.25±0.03mm, n=39 offspring, P=4.6E-11); there was a trend toward slightly worsened healing compared to primary MRL-transplanted B6 mice (0.63±0.03mm vs. 0.74±0.05mm, P=0.092) (**Table 1, Figure 1E**). There were no differences in healing among offspring where both sire and dam were transplanted compared to sire-only or dam-only-transplanted offspring (both transplanted: 0.65±0.02mm, n=4, vs. one transplanted: 0.63±0.03, n=35, P=0.61).

Durable gut microbiome alterations following microbiome transplantation, and microbiome clade associations with earhole closure rates

Next, we profiled the cecal microbiomes of 43 animals, including 8 B6-vehicle (4 male and 4 female), 8 MRL-transplanted B6 (4 male and 4 female), 8 MRL-vehicle (4 male and 4 female), and 19 offspring of MRL-transplanted B6 mice (11 male and 8 female). All samples demonstrated high 16S sequencing quality, with raw OTU counts per sample ranging from 123,543 to 456,880. There were no statistically significant differences in raw OTU counts among any group.

First, we analyzed alpha diversity, a measure of the overall number of bacterial clades present per group, using the observed OTU method following rarefaction to the lowest OTU count (**Figure 2A**). MRL-vehicle samples demonstrated significantly higher alpha diversity than the other groups (MRL-vehicle 736±15 mean OTUs vs. B6-vehicle 603±30, P=0.0014, MRL-vehicle vs. MRL-transplanted B6 636±32, P=0.013, MRL-vehicle vs. offspring of MRL-transplanted B6 615±12, P=5.44E-6). There were no statistically significant differences in alpha diversity among B6-vehicle, MRL-

transplanted B6, and offspring of MRL-transplanted B6 mice. Beta diversity, a measure of diversity in the composition of groups, was then computed by the permanova method; we saw significant differences (*P*<0.001) among all groups (**Figure 2B**).

We found numerous differences in cecal microbial clades when comparing mouse groups (**Figure 2C**). In B6-vehicle vs. MRL-vehicle groups, 57 clades were significantly different **(Supplemental Table 2)**, in B6-vehicle vs. MRL-transplanted B6 groups, 17 clades were different **(Supplementary Table 3)**, in MRL-vehicle vs. B6-transplanted MRL groups, 239 clades were different **(Supplementary Table 4)**, and finally, comparing progeny of MRL-transplanted B6 mice to B6-vehicle mice, we found 55 differences **(Supplementary Table 5)**. A number of clade differences were shared among the various groups; for example, members of phylum *Verrucomicrobia*, particularly genus *Akkermansia*, were consistently characteristic of B6 mice or mice transplanted with B6 cecal content (LDA-ES 4.46, *P*=0.0008 in MRL-vehicle vs. B6-vehicle comparisons; LDA-ES 4.23 with *P*=0.0008 in MRL-transplanted B6 vs. B6-vehicle comparisons, LDA-ES 3.84, *P*=0.04 in progeny vs. B6-vehicle, and LDA-ES 4.37 with *P*=0.0008 in B6-transplanted MRL vs. MRL-vehicle comparisons). Conversely, phylum *Firmicutes* was consistently associated with MRL or MRL-transplanted animals (LDA-ES 4.71, *P*=7.8E-4 in MRL-vehicle vs. B6-vehicle; LDA-ES 4.22, *P*=0.003 in progeny vs. B6-vehicle; LDA-ES 4.56, *P*=7.8E-4 in B6-transplanted MRL vs. MRL-vehicle). Within phylum *Firmicutes*, members of order *Clostridiales* were characteristic of MRL or MRL-transplanted animals (LDA-ES 4.32, *P*=7.8E-4 in MRL-vehicle vs. B6-vehicle; LDA-ES 3.76, *P*=0.04; LDA-ES 4.42, *P*=7.8E-4 in B6-transplanted MRL vs.

MRL-vehicle), as were members of order *Lactobacillales* (LDA-ES 2.80, *P*=7.8E-4 in MRL-vehicle vs. B6-vehicle; LDA-ES 3.89, *P*=0.002 in MRL-transplanted B6 vs. B6-vehicle). Comparing B6-transplanted MRL to MRL-vehicle mice, we identified the transfer of B6-associated clades into recipient animals, including members of phylum *Verrucomicrobiae* (LDA-ES 4.40, *P*=7.8E-4), whereas MRL-vehicle animals were again characterized by members of the phylum *Firmicutes* (LDA-ES 4.56, *P*=7.8E-4), among others. We then correlated microbial clades to individual earhole closure rates. We found 44 clades highly correlated **(Figure 2D, Supplementary Table 6)**, including positive correlations with phylum *Firmicutes* (R=0.76, *P*=5.8E-8), order *Clostridiales* (R=0.72, P=7.5E-7), and order *Lactobacillales* (R=0.55, *P*=5.4E-4). Negative correlations with earhole closure rates were seen among phylum *Verrucomicrobia*, specifically genus *Akkermansia* (R=-0.71, *P*=1E-6) and order *Burkholderiales* (R=-0.58, *P*=1.7E-4).

We next examined the Gram status of cecal contents in the present experiment. We found a decrease in Gram-negative constituent organisms in groups with improved ear healing (B6-vehicle fraction cecal reads Gram-negative 0.39±0.02 vs. MRL-transplanted B6 0.23±0.03 vs. MRL-vehicle 0.06±0.01, B6-vehicle vs. MRL-vehicle *P*=3.6E-9, B6-vehicle vs. MRL-transplanted B6 *P*=1.4E-5). However, offspring of MRL-transplanted B6 mice did not demonstrate a significant shift in microbiome Gram status (Offspring: 0.37±0.03, *P*=0.7 vs. B6-vehicle). Nonetheless, individual Gram-negative bacterial fraction was negatively correlated with individual earhole closure rates (**Figure 2E**, R=-0.67, *P*=3.6E-6).

Sex disparities in earhole closure rates, and correlations with gut microbiome constituents

Female mice are less affected by surgically induced OA than are male mice [43]. As our study included both sexes, we evaluated sex-related differences in earhole closure in control and transplanted mice, as well as any shared, sex-related microbiome differences that might underlie earhole closure variations. Earhole closure rates in MRL-transplanted B6 mice were not affected by the sex of the MRL donor mouse (*P*=0.61), nor were rates in B6-transplanted MRL mice affected by the sex of the B6 donor mouse (*P*=0.33). However, we did find variation in earhole closure rates depending on the sex of the recipient mouse **(Figure 3A)**. Female B6-vehicle demonstrated a trend towards an improved healing response (*P*=0.059), with a similar trend found in female MRL-transplanted B6 mice (*P*=0.096). Differences were seen in both female B6-transplanted MRL and female MRL-vehicle mice, where healing was significantly better than their male counterparts (*P*=0.0015 and P=4.2E-6 for B6-transplanted MRL and MRL-vehicle mice respectively). Furthermore, in heritability experiments, found a roughly one-third improvement in healing among female offspring compared to male offspring (*P*=0.0038, **Figure 3A**).

For cecal 16S analysis, we pooled microbiome data from B6-vehicle, MRL-vehicle, and MRL-transplanted B6 animals and compared by sex. We first evaluated alpha diversity using the observed OTU method following rarefaction, as previously described, and did not find any sex-related differences (males: 646±13 vs. females: 632±21, *P* = 0.57). We

found differences in beta diversity by sex both within mouse transplant groups (all *P*<0.001), and when all animals were considered together (*P*=0.012) (**Figure 3B**). We then analyzed our 16S data by pooling all animals from the above groups and comparing male to female animals. We found 18 clades which were different between the groups **(Figure 3C)**; among these, many were shared with those clades identified as differentiating MRL and B6 animals, above. These included phylum *Verrucomicrobia* (increased in males, LDA-ES 3.88, *P* = 0.02) and order *Clostridiales* (increased in females, LDA-ES 3.99, *P*=0.01) **(Supplementary Table 7)**.

Imputed functional analysis of earhole closure-associated gut microbiome changes

To offer insight into bacterial metabolomic and metagenomic changes associated with transplantation, we next imputed cecal microbiome metagenomic function using the Phylogenetic Investigation of Communities by Reconstruction of Unobserved States (PICRUSt) analysis package (40). We compared MRL-transplanted B6 to B6-vehicle groups and identified 218 Kyoto Encyclopedia of Gene and Genomes (KEGG) pathways altered within gut microbiota (**Supplementary Table 8**) at an FDR threshold of *P*≤0.01. Of these, 48 were highly correlated with earhole closure rates (*P*≤0.01) (**Table 2**). The strongest positive correlations included D-arginine and D-ornithine metabolism (R=0.73, *P*=0.007), flavone and flavonol biosynthesis (R=0.72, *P*=0.005), and mineral absorption (R=0.66, *P*=0.003), whereas negative correlations included beta-lactam resistance (R=-0.78, *P*=0.003), penicillin and cephalosporin biosynthesis (R=-0.78, *P*=6E-4), glycosphingolipid biosynthesis (R=-0.75, *P*=6E-4), and lipopolysaccharide biosynthesis (R=-0.73, *P*=5E-4), among others.

Discussion:

In this study, we provide the first evidence that the spontaneous earhole phenotype seen in MRL/MpJ mice is associated with specific gut microbiome constituents and is transferable to nonhealer B6 mice via gut microbiome transplantation. Furthermore, we describe novel sex discrepancies in earhole closure rates in B6 and MRL mice, where female animals demonstrate improved healing compared to males. We find that transplant-associated improvements in earhole wound closure are time dependent, and that the best outcomes are achieved if gut microbiome transplantation occurs before ear wounding. Intriguingly, offspring of MRL-transplanted B6 mice also demonstrate improved healing compared to non-transplanted controls, indicating transgenerational heritability. In cecal microbiome 16S sequencing analysis, we identified a number of clades that are associated, both positively and negatively, with ear wound healing, including phylum *Firmicutes*, order *Clostridiales*, order *Lactobacillales*, and phylum *Verrucomicrobia*. We also found a negative association between Gram-negative organisms and ear wound healing despite an increase in serum LPS levels in both MRL and MRL-transplanted B6 animals.

These data offer a counterpoint to the prevailing dogma that the superhealing characteristics of MRL mice are purely genetic in origin, as we demonstrate that roughly half of the MRL-associated wound healing capacity can be transferred to nonhealer mice via a single gut microbiome transplantation. We did not see a reduction in ear

wound healing capability of MRL mice following transplantation of a B6 microbiome despite confirming a reduction in key healing-associated gut microbiome clades in B6-transplanted animals, suggesting the microbiome is not the sole determinant of earhole closure. Furthermore, although we noted transgenerational heritability of both the earhole closure phenotype and cecal microbiota clades of MRL-transplanted B6 mice, we saw a trend towards reduction of earhole closure in offspring compared to primary transplanted animals (P=0.09), as well as a reversion of Gram-negative gut constituents in offspring towards a 'baseline' B6 phenotype, suggesting that both the transplant-associated microbiome changes and cartilage healing phenotype may be lost over multiple generations. This raises the intriguing possibility that the unique genetic makeup of MRL mice is itself leading to alterations of the gut microbiome, perhaps through divergent immune responses within the gut, which subsequently contributes to the earhole closure phenotype.

We also unexpectedly identified differences between male and female animals in both earhole closure rates and gut microbiome constituent organisms. Previous studies have highlighted a reduction in OA histopathologic severity in female mice, in both young and old animals [43,44]. Although not evaluated directly in the context of OA, sex-specific differences in the gut microbiome have been described in association with known OA risk factors, including high fat diet-induced obesity [45,46] and advanced age [47]. In the present study, our 16S analysis identified 18 sex-associated microbiome clades; among these, 7 overlapped with our MRL vs. B6 comparison. In every case, healing-associated clades were enriched in females, whereas nonhealing-associated clades were enriched

in males. If our earhole closure phenotype indeed correlates with protection from OA in transplanted animals (to be evaluated in future studies), microbiome differences might offer a novel explanation for differences in sex-associated OA risk un mice. In this regard, our confirmation that the gut microbiome-mediated earhole closure phenotype is stable even when transplanting adult animals bodes well for future studies of murine OA prevention.

Relatively few studies have rigorously evaluated the microbiome in the context of human cartilage regeneration through studies on OA. The largest to date, published in 2019 by Boer et al., found four bacterial clades associated with knee pain among 867 adults within the Dutch Rotterdam (RSIII) and LifeLines-DEEP OA cohorts [48]. These included class *Bacilli*, order *Lactobacillales*, family *Streptococcaceae*, and genus *Streptococcus.* In the present study, we found members of order *Lactobacillales* within the gut are strongly associated with ear wound healing in MRL-transplanted B6 mice, as well as one of the clades transgenerationally inherited to progeny of MRL-transplanted B6 mice. *Lactobacillus* has been shown to be depleted within the gut during mouse aging [49], a known risk factor for OA development. These findings align with our previous work which identified *Lactobacillales* DNA as characteristic of both disease-free human control and OA-protected MRL cartilage [50]. Similarly, we found family *Clostridiaceae* within cecal microbiota to be highly correlated with ear wound healing, and we previously identified this clade as associated with disease-free human cartilage. Members of the order *Burkholderiales* were strongly negatively correlated with earhole closure; this order was associated with OA cartilage in our previous study. In 2019, Rios

et al. published a report of decreased OA severity in a rat model following supplementation of a high fat/high sucrose diet with prebiotic fiber; in their model, fiber treatment increased *Bifidobacterium* and *Roseburia* and decreased *Clostridium* and *Akkermansia* [51]. In our data, *Akkermansia* (within phylum *Verrucomicrobia*) was associated with poor healing, corroborating these findings.

The transgenerational heritability we identified in this study is interesting; previous reports have identified transgenerational heritability of microbiome-mediated inflammatory conditions [52], and a paper in 2020 demonstrated transgenerational heritability of weight gain, metabolic imbalance, and injury-induced OA for at least 2 generations following high-fat diet treatment in mice [53]. Unfortunately, this study did not evaluate the microbiome as a potential mediator of these effects. A number of studies have proposed an interaction between the gut microbiome and host epigenetic mechanisms in mediating transgenerational effects [54,55]

Despite the associations we have described in this study, the key unanswered question is the mechanism driving cecal microbiome-mediated ear wound healing, which will no doubt require substantial future investigation to unravel. It is possible that alterations in the gut microbiome, through transplantation, may have induced systemic alterations in microbial metabolites and lead to a generalized pro-healing environment. Conversely, the metabolites of certain gut organisms, particularly short-chain fatty acids (SCFA), can promote intestinal repair and wound healing locally by inducing healing-associated gene expression in epithelial cells [56]. Another possible explanation would be the alteration

of the cutaneous microbiome at the site of wounding, presumably via fecal-skin inoculation. Previous studies have indicated that altered skin flora plays a role in impaired cutaneous healing [57–59], principally related to biofilm formation at the wound site, with an associated increase in inflammatory cytokine production, limiting healing capacity [60].

Although we did not evaluate microbial metabolites directly, we did gain insight into metabolite alterations indirectly through our imputed functional metagenomic analysis. We found a variety of imputed KEGG pathways associated with earhole closure, including a few with previous links to tissue regeneration/healing and OA development. These included an association with flavone biosynthesis, previously associated with promotion of wound healing in rats [61] and suggested as an anti-inflammatory agent for use in OA (by reduction in NF-KB and MAPK activation) [62]. We also saw an association with D-arginine and D-ornithine metabolism, both enhancers of wound healing in mice [63,64]; intriguingly, there is some evidence that plasma arginine levels are reduced in knee OA patients [65]. Additional associations of interest include fatty acid elongation; serum fatty acid chain length is associated with symptomatic end-stage OA [66], and the bacterial secretion system, which enables the export of bacterial proteases to the extracellular environment in the context of chronic wound establishment [67].

Finally, our finding of differences in earhole closure rates of animals raised in-house vs. those purchased from a commercial vendor and immediately used is in line with

previous reports of cecal microbiome changes associated with various animal vendors [41,42]. This observation also reinforces the potential for variation in microbiome-linked phenotypic changes like earhole closure related to geographic location and diet; researchers should keep this in mind when designing future microbiome-related experiments.

Our study has several limitations. First, performed transplantation of animals with an already-existing microbiota rather than colonizing germ-free animals. Although using non-germ-free animals introduces the possibility of confounding results by variations in transplant engraftment, it also makes our study more compelling from a potential human therapeutic perspective. Another limitation is our lack of a definitive mechanistic explanation for the healing that we describe, this will no doubt require an extensive evaluation of several factors including local and systemic inflammatory responses, previously associated with healing in MRL mice [68], and cell cycle/DNA damage response, also associated with healing in MRL and $p21^{-/-}$ mice [69]. Nevertheless, we felt that a timely publication of our observations was necessary to spur further research in this area. Finally, we limited our study to one spontaneous healer strain (MRL) and analyzed only young and young-adult mice; future analyses should include other strains and expand to evaluate the transplant-associated healing potential, if any, in older mice.

In summary, herein we offer the first description of the gut microbiome-associated nature of the earhole cartilage healing phenotype previously described in MRL/MpJ mice, and demonstrate that this trait can be conferred to nonhealer mice via a gut

microbiome transplantation. We identified several clades within the gut microbiome that are strongly associated (both positively and negatively) with earhole closure, and demonstrate that transgenerational inheritance of transplanted gut microbiome constituents and microbiome-mediate earhole closure occurs. Furthermore, we found evidence for sex-specific effects of both earhole closure and gut microbiome trends, with female animals healing better than males in a variety of contexts. Finally, we identified a number of differences in imputed metagenomes among healing-associated microbiome clades. Future work should focus on determining the mechanism underlying this microbiome-associated healing phenotype and expanding this analysis to include other animals identified as superhealers, including LG/J mice, *Acomys* mice, and perhaps invertebrate healers. The potential for a gut microbiome-mediated healing response should also be evaluated in the context of OA, which may offer a unique avenue for future therapeutic development.

Table 1: Earhole closure rates 4 weeks after a 2.0mm ear punch under various cecal transplantation conditions

Primary microbiome transplantation					
Mouse group	**N**	**Earhole closure (mm)**	**Earhole closure P values vs. (sex-matched) B6-vehicle**	**Earhole closure P values vs. (sex matched) MRL-vehicle**	**Earhole closure P values, male vs. female**
B6-vehicle	**25**	**0.25±0.03**		**6.9E-10**	**0.059**
Females	12	0.31±0.04		1.7E-10	
Males	13	0.19±0.04		1.5E-12	
MRL-transplanted B6	**36**	**0.74±0.05**	**6.9E-10**	**1.8E-12**	**0.096**
Females	18	0.82±0.09	1.8E-7	2.5E-7	
Males	18	0.65±0.05	8.0E-5	1.8E-7	
B6-transplanted MRL	**21**	**1.28±0.10**		**0.20**	**1.6E-6**
Females	8	1.77±0.06		0.13	
Males	13	0.99±0.08		0.025	
MRL-vehicle	**28**	**1.40±0.07**	**6.9E-10**		**0.0031**
Females	15	1.49±0.10	4.0E-13		
Males	13	1.30±0.08	2.4E-12		
Heritability: earhole closure results of MRL-transplanted B6 mouse offspring					

Mouse group	N	Earhole closure (mm)	Earhole closure P values vs.(sex-matched) B6-vehicle	Earhole closure P values vs.(sex matched) primary MRL-transplanted B6	Earhole closure P values, male vs. female
Offspring of MRL-transplanted B6	**39**	**0.63±0.03**	**4.6E-11**	**0.092**	**0.0038**
Sire + Dam transplanted	4	0.65±0.02	1.8E-5	0.71	
Dam only transplanted	23	0.65±0.04	1.1E-8	0.25	
Sire only transplanted	12	0.60±0.07	5.1E-6	0.16	
Female offspring	20	0.73±0.04	6.4E-7	0.35	
Male offspring	19	0.54±0.05	1.5E-6	0.10	

Table 2: Top imputed microbiome metagenomes correlated with earhole closure rates among B6-vehicle, MRL-transplanted B6, and MRL-vehicle mouse groups.

KEGG pathway correlated with earhole closure	Pearson R value	*P* value of correlation
Beta-Lactam resistance	-0.78	0.003
Penicillin and cephalosporin biosynthesis	-0.78	6E-4
1,1,1-Trichloro-2,2-bis(4-chlorophenyl)ethane (DDT) degradation	-0.77	0.008
Glycosphingolipid biosynthesis - ganglio series	-0.75	6E-4
Lipopolysaccharide biosynthesis	-0.73	5E-4
Meiosis - yeast	-0.73	4E-4
Fatty acid elongation in mitochondria	-0.73	4E-4
Proximal tubule bicarbonate reclamation	-0.73	3E-4
Caffeine metabolism	-0.73	4E-4
Fluorobenzoate degradation	-0.73	4E-4
Circadian rhythm - plant	-0.73	4E-4
Steroid biosynthesis	-0.73	4E-4

Ubiquitin system	-0.72	5E-4
Primary immunodeficiency	0.56	0.004
Basal transcription factors	0.61	0.004
Mineral absorption	0.66	0.003
Flavone and flavonol biosynthesis	0.72	0.005
D-Arginine and D-ornithine metabolism	0.73	0.006

Figure Legends:

Figure 1: Mouse earhole closure results 4 weeks after a 2.0mm ear punch under various microbiome conditions. **(A)** Earhole closure in transplanted mice at weaning. Line represents mean, whiskers represent SEM. **(B)** Earhole closure in MRL-transplanted B6 mice, where transplantation occurred at various times relative to earhole punch. **(C)** Comparison of earhole closure in MRL-transplanted B6 mice, where transplants were performed at weaning (3-4 weeks of age) vs. as adults (12 weeks of age). **(D)** Differences in earhole closure rates in mice (donors and recipients) raised in-house compared to those purchased from a commercial vendor (Jackson laboratories) and immediately used. **(E)** Earhole closure of MRL-transplanted B6 mice compared to offspring of MRL-transplanted B6 mice.

Figure 2: 16S deep sequencing analysis of cecal samples. **(A)** Alpha diversity by observed OUT method following rarefaction of transplantation mouse groups. Dot represents mean, lines represent SEM. **(B)** Beta diversity plot by weighted unifrac method of mouse 16S samples by group. **(C)** Statistically significant differences in cecal microbiome composition in various mouse groups. Bars represent linear discriminant analysis (LDA) effect size scores. **(D)** Plots of cecal clades most strongly correlated with individual earhole closure rates. B6-vehicle, MRL-vehicle, MRL-transplanted B6, and progeny of MRL-transplanted B6 mice included. **(E)** Cecal microbiome Gram negative proportion data, including dot plot (line represents mean, whiskers represent SEM) and linear correlation. B6-vehicle, MRL-vehicle, MRL-transplanted B6, and progeny of MRL-transplanted B6 mice included.

Figure 3: Disparities in mouse earhole closure and cecal microbiome analysis by mouse sex. **(A)** Earhole closure results separated by sex, lines represent mean, whiskers represent SEM. **(B)** Beta diversity plot of mice by weighted unifrac method, colors represent mouse sex. **(C)** Statistically significant differences in cecal microbiome composition by sex. Bars represent linear discriminant analysis (LDA) effect size scores.

References:

1. Murphy ED, Roths JB. Autoimmunity and lymphoproliferation: induction by mutant gene lpr, and acceleration by a male-associated factor in strain BXSB mice. 1978; 207.

2. Adachi M, Watanabe-Fukunaga R, Nagata S. Aberrant transcription caused by the insertion of an early transposable element in an intron of the Fas antigen gene of lpr mice. Proc Natl Acad Sci U S A. 1993;90: 1756–1760.

3. Clark LD, Clark RK, Heber-Katz E. A new murine model for mammalian wound repair and regeneration. Clin Immunol Immunopathol. 1998;88: 35–45.

4. Heber-Katz E. The regenerating mouse ear. Semin Cell Dev Biol. 1999;10: 415–419.

5. Chadwick RB, Bu L, Yu H, Hu Y, Wergedal JE, Mohan S, et al. Digit tip regrowth and differential gene expression in MRL/Mpj, DBA/2, and C57BL/6 mice. Wound Repair Regen. 2007;15: 275–284.

6. Han M, Yang X, Taylor G, Burdsal CA, Anderson RA, Muneoka K. Limb regeneration in higher vertebrates: developing a roadmap. Anat Rec B New Anat. 2005;287: 14–24.

7. Buckley G, Metcalfe AD, Ferguson MWJ. Peripheral nerve regeneration in the MRL/MpJ ear wound model. J Anat. 2011;218: 163–172.

8. Leferovich JM, Bedelbaeva K, Samulewicz S, Zhang XM, Zwas D, Lankford EB, et al. Heart regeneration in adult MRL mice. Proc Natl Acad Sci U S A. 2001;98: 9830–9835.

9. Naseem RH, Meeson AP, Michael Dimaio J, White MD, Kallhoff J, Humphries C, et al. Reparative myocardial mechanisms in adult C57BL/6 and MRL mice following injury. Physiol Genomics. 2007;30: 44–52.

10. Hrbek T, de Brito RA, Wang B, Pletscher LS, Cheverud JM. Genetic characterization of a new set of recombinant inbred lines (LGXSM) formed from the intercross of SM/J and LG/J inbred mouse strains. Mamm Genome. 2006;17: 417.

11. Rai MF, Hashimoto S, Johnson EE, Janiszak KL, Fitzgerald J, Heber-Katz E, et al. Heritability of articular cartilage regeneration and its association with ear wound healing in mice. Arthritis Rheum. 2012;64: 2300–2310.

12. Rai MF, Sandell LJ. Regeneration of articular cartilage in healer and non-healer mice. Matrix Biol. 2014;39: 50–55.

13. Li X, Gu W, Masinde G, Hamilton-Ulland M, Xu S, Mohan S, et al. Genetic control of the rate of wound healing in mice. Heredity . 2001;86: 668–674.

14. Blankenhorn EP, Bryan G, Kossenkov AV, Clark LD, Zhang X-M, Chang C, et al. Genetic

loci that regulate healing and regeneration in LG/J and SM/J mice. Mamm Genome. 2009;20: 720–733.

15. Masinde G, Li X, Baylink DJ, Nguyen B, Mohan S. Isolation of wound healing/regeneration genes using restrictive fragment differential display-PCR in MRL/MPJ and C57BL/6 mice. Biochem Biophys Res Commun. 2005;330: 117–122.

16. Rai MF, Schmidt EJ, McAlinden A, Cheverud JM, Sandell LJ. Molecular insight into the association between cartilage regeneration and ear wound healing in genetic mouse models: targeting new genes in regeneration. G3 . 2013;3: 1881–1891.

17. Gurtner GC, Werner S, Barrandon Y, Longaker MT. Wound repair and regeneration. Nature. 2008. pp. 314–321. doi:10.1038/nature07039

18. Leonard CA, Lee W-Y, Tailor P, Salo PT, Kubes P, Krawetz RJ. Allogeneic Bone Marrow Transplant from MRL/MpJ Super-Healer Mice Does Not Improve Articular Cartilage Repair in the C57Bl/6 Strain. PLoS One. 2015;10: e0131661.

19. Chinzei N, Rai MF, Hashimoto S, Schmidt EJ, Takebe K, Cheverud JM, et al. Evidence for Genetic Contribution to Variation in Posttraumatic Osteoarthritis in Mice. Arthritis & Rheumatology. 2019;71: 370–381.

20. Fitzgerald J, Rich C, Burkhardt D, Allen J, Herzka AS, Little CB. Evidence for articular cartilage regeneration in MRL/MpJ mice. Osteoarthritis Cartilage. 2008;16: 1319–1326.

21. Sharma A, Kudesia P, Shi Q, Gandhi R. Anxiety and depression in patients with osteoarthritis: impact and management challenges. Open Access Rheumatol. 2016;8: 103–113.

22. Swain S, Sarmanova A, Coupland C, Doherty M, Zhang W. Comorbidities in Osteoarthritis: A systematic review and meta-analysis of observational studies. Arthritis Care Res . 2019. Available: https://onlinelibrary.wiley.com/doi/abs/10.1002/acr.24008

23. Wang H, Bai J, He B, Hu X, Liu D. Osteoarthritis and the risk of cardiovascular disease: a meta-analysis of observational studies. Sci Rep. 2016;6: 39672.

24. Centers for Disease Control and Prevention (CDC). Prevalence of doctor-diagnosed arthritis and arthritis-attributable activity limitation--United States, 2010-2012. MMWR Morb Mortal Wkly Rep. 2013;62: 869–873.

25. Lleal M, Sarrabayrouse G, Willamil J, Santiago A, Pozuelo M, Manichanh C. A single faecal microbiota transplantation modulates the microbiome and improves clinical manifestations in a rat model of colitis. EBioMedicine. 2019. doi:10.1016/j.ebiom.2019.10.002

26. Manichanh C, Reeder J, Gibert P, Varela E, Llopis M, Antolin M, et al. Reshaping the gut microbiome with bacterial transplantation and antibiotic intake. Genome Res. 2010;20: 1411–1419.

27. 16S Sample Preparation Guide. Available: https://support.illumina.com/documents/documentation/chemistry_documentation/16s/16s-metagenomic-library-prep-guide-15044223-b.pdf

28. Caporaso JG, Kuczynski J, Stombaugh J, Bittinger K, Bushman FD, Costello EK, et al.

QIIME allows analysis of high-throughput community sequencing data. Nat Methods. 2010;7: 335–336.

29. Edgar RC. Search and clustering orders of magnitude faster than BLAST. Bioinformatics. 2010;26: 2460–2461.

30. McDonald D, Price MN, Goodrich J, Nawrocki EP, DeSantis TZ, Probst A, et al. An improved Greengenes taxonomy with explicit ranks for ecological and evolutionary analyses of bacteria and archaea. ISME J. 2012;6: 610–618.

31. Chang Q, Luan Y, Sun F. Variance adjusted weighted UniFrac: a powerful beta diversity measure for comparing communities based on phylogeny. BMC Bioinformatics. 2011;12: 118.

32. Hamady M, Knight R. Microbial community profiling for human microbiome projects: Tools, techniques, and challenges. Genome Res. 2009;19: 1141–1152.

33. Segata N, Izard J, Waldron L, Gevers D, Miropolsky L, Garrett WS, et al. Metagenomic biomarker discovery and explanation. Genome Biol. 2011;12: R60.

34. Kruskal WH, Wallis WA. Use of Ranks in One-Criterion Variance Analysis. J Am Stat Assoc. 1952;47: 583–621.

35. Fisher RA. THE USE OF MULTIPLE MEASUREMENTS IN TAXONOMIC PROBLEMS. Ann Eugen. 1936;7: 179–188.

36. Battaglia T. LEfSe · An Introduction to QIIME 1.9.1. [cited 14 Feb 2018]. Available: https://twbattaglia.gitbooks.io/introduction-to-qiime/content/lefse.html

37. Langille MGI, Zaneveld J, Caporaso JG, McDonald D, Knights D, Reyes JA, et al. Predictive functional profiling of microbial communities using 16S rRNA marker gene sequences. Nat Biotechnol. 2013;31: 814–821.

38. Kanehisa M, Goto S. KEGG: kyoto encyclopedia of genes and genomes. Nucleic Acids Res. 2000;28: 27–30.

39. Parks DH, Tyson GW, Hugenholtz P, Beiko RG. STAMP: statistical analysis of taxonomic and functional profiles. Bioinformatics. 2014;30: 3123–3124.

40. Le Roy T, Debédat J, Marquet F, Da-Cunha C, Ichou F, Guerre-Millo M, et al. Comparative Evaluation of Microbiota Engraftment Following Fecal Microbiota Transfer in Mice Models: Age, Kinetic and Microbial Status Matter. Front Microbiol. 2018;9: 3289.

41. Rasmussen TS, de Vries L, Kot W, Hansen LH, Castro-Mejía JL, Vogensen FK, et al. Mouse Vendor Influence on the Bacterial and Viral Gut Composition Exceeds the Effect of Diet. Viruses. 2019;11. doi:10.3390/v11050435

42. Ericsson AC, Davis JW, Spollen W, Bivens N, Givan S, Hagan CE, et al. Effects of vendor and genetic background on the composition of the fecal microbiota of inbred mice. PLoS One. 2015;10: e0116704.

43. Ma H-L, Blanchet TJ, Peluso D, Hopkins B, Morris EA, Glasson SS. Osteoarthritis severity is sex dependent in a surgical mouse model. Osteoarthritis Cartilage. 2007;15: 695–700.

44. Huang H, Skelly JD, Ayers DC, Song J. Age-dependent Changes in the Articular Cartilage and Subchondral Bone of C57BL/6 Mice after Surgical Destabilization of Medial Meniscus. Sci Rep. 2017;7: 42294.

45. Peng C, Xu X, Li Y, Li X, Yang X, Chen H, et al. Sex-specific association between the gut microbiome and high-fat diet-induced metabolic disorders in mice. Biol Sex Differ. 2020;11: 5.

46. Min Y, Ma X, Sankaran K, Ru Y, Chen L, Baiocchi M, et al. Sex-specific association between gut microbiome and fat distribution. Nature Communications. 2019. doi:10.1038/s41467-019-10440-5

47. Wang J, Lang T, Shen J, Dai J, Tian L, Wang X. Core Gut Bacteria Analysis of Healthy Mice. Front Microbiol. 2019;10: 887.

48. Boer CG, Radjabzadeh D, Medina-Gomez C, Garmaeva S, Schiphof D, Arp P, et al. Intestinal microbiome composition and its relation to joint pain and inflammation. Nat Commun. 2019;10: 4881.

49. Langille MG, Meehan CJ, Koenig JE, Dhanani AS, Rose RA, Howlett SE, et al. Microbial shifts in the aging mouse gut. Microbiome. 2014;2: 50.

50. Dunn CM, Velasco C, Rivas A, Andrews M, Garman C, Jacob PB, et al. Identification of cartilage microbial DNA signatures and associations with knee and hip osteoarthritis. Arthritis Rheumatol. 2020. doi:10.1002/art.41210

51. Rios JL, Bomhof MR, Reimer RA, Hart DA, Collins KH, Herzog W. Protective effect of prebiotic and exercise intervention on knee health in a rat model of diet-induced obesity. Sci Rep. 2019;9: 3893.

52. Soderborg TK, Clark SE, Mulligan CE, Janssen RC, Babcock L, Ir D, et al. The gut microbiota in infants of obese mothers increases inflammation and susceptibility to NAFLD. Nature Communications. 2018. doi:10.1038/s41467-018-06929-0

53. Harasymowicz NS, Choi Y-R, Wu C-L, Iannucci L, Tang R, Guilak F. Intergenerational transmission of diet-induced obesity, metabolic imbalance, and osteoarthritis in mice. Arthritis Rheumatol. 2019. doi:10.1002/art.41147

54. Romano KA, Martinez-del Campo A, Kasahara K, Chittim CL, Vivas EI, Amador-Noguez D, et al. Metabolic, epigenetic, and transgenerational effects of gut bacterial choline consumption. Cell Host Microbe. 2017;22: 279-290.e7.

55. Marques FZ. Missing heritability of hypertension and our microbiome. Circulation. 2018;138: 1381–1383.

56. Bilotta AJ, Ma C, Huang X, Yang W, Chen L, Yao S, et al. Microbiota metabolites SCFA promote intestinal epithelial repair and wound healing through promoting epithelial cell production of milk fat globule-EGF factor 8. The Journal of Immunology. 2018;200: 53.17-53.17.

57. James GA, Swogger E, Wolcott R, Pulcini ED, Secor P, Sestrich J, et al. Biofilms in chronic wounds. Wound Repair Regen. 2008;16: 37–44.

58. Wolcott RD, Hanson JD, Rees EJ, Koenig LD, Phillips CD, Wolcott RA, et al. Analysis of the chronic wound microbiota of 2,963 patients by 16S rDNA pyrosequencing. Wound Repair Regen. 2016;24: 163–174.

59. Johnson TR, Gómez BI, McIntyre MK, Dubick MA, Christy RJ, Nicholson SE, et al. The Cutaneous Microbiome and Wounds: New Molecular Targets to Promote Wound Healing. Int J Mol Sci. 2018;19. doi:10.3390/ijms19092699

60. Secor PR, James GA, Fleckman P, Olerud JE, McInnerney K, Stewart PS. Staphylococcus aureus Biofilm and Planktonic cultures differentially impact gene expression, mapk phosphorylation, and cytokine production in human keratinocytes. BMC Microbiology. 2011. p. 143. doi:10.1186/1471-2180-11-143

61. Gupta A, Kumar R, Pal K, Singh V, Banerjee PK, Sawhney RC. Influence of sea buckthorn (Hippophae rhamnoides L.) flavone on dermal wound healing in rats. Mol Cell Biochem. 2006;290: 193–198.

62. Ferraz CR, Carvalho TT, Manchope MF, Artero NA, Rasquel-Oliveira FS, Fattori V, et al. Therapeutic Potential of Flavonoids in Pain and Inflammation: Mechanisms of Action, Pre-Clinical and Clinical Data, and Pharmaceutical Development. Molecules. 2020;25. doi:10.3390/molecules25030762

63. Shi HP, Fishel RS, Efron DT, Williams JZ, Fishel MH, Barbul A. Effect of supplemental ornithine on wound healing. J Surg Res. 2002;106: 299–302.

64. Shi HP, Efron DT, Most D, Tantry US, Barbul A. Supplemental dietary arginine enhances wound healing in normal but not inducible nitric oxide synthase knockout mice. Surgery. 2000;128: 374–378.

65. Zhang W, Sun G, Likhodii S, Liu M, Aref-Eshghi E, Harper PE, et al. Metabolomic analysis of human plasma reveals that arginine is depleted in knee osteoarthritis patients. Osteoarthritis Cartilage. 2016;24: 827–834.

66. Meessen JMTA, Saberi-Hosnijeh F, Bomer N, den Hollander W, van der Bom JG, van Hilten JA, et al. Serum fatty acid chain length associates with prevalent symptomatic end-stage osteoarthritis, independent of BMI. Sci Rep. 2020;10: 15459.

67. Suleman L. Extracellular Bacterial Proteases in Chronic Wounds: A Potential Therapeutic Target? Adv Wound Care. 2016;5: 455–463.

68. Ward BD, Furman BD, Huebner JL, Kraus VB, Guilak F, Olson SA. Absence of posttraumatic arthritis following intraarticular fracture in the MRL/MpJ mouse. Arthritis Rheum. 2008;58: 744–753.

69. Bedelbaeva K, Snyder A, Gourevitch D, Clark L, Zhang X-M, Leferovich J, et al. Lack of p21 expression links cell cycle control and appendage regeneration in mice. Proc Natl Acad Sci U S A. 2010;107: 5845–5850.

Figure 1: Mouse earhole closure results 4 weeks after a 2.0mm ear punch under various microbiome transplantation conditions

A. Earhole closure results, mice transplanted at weaning

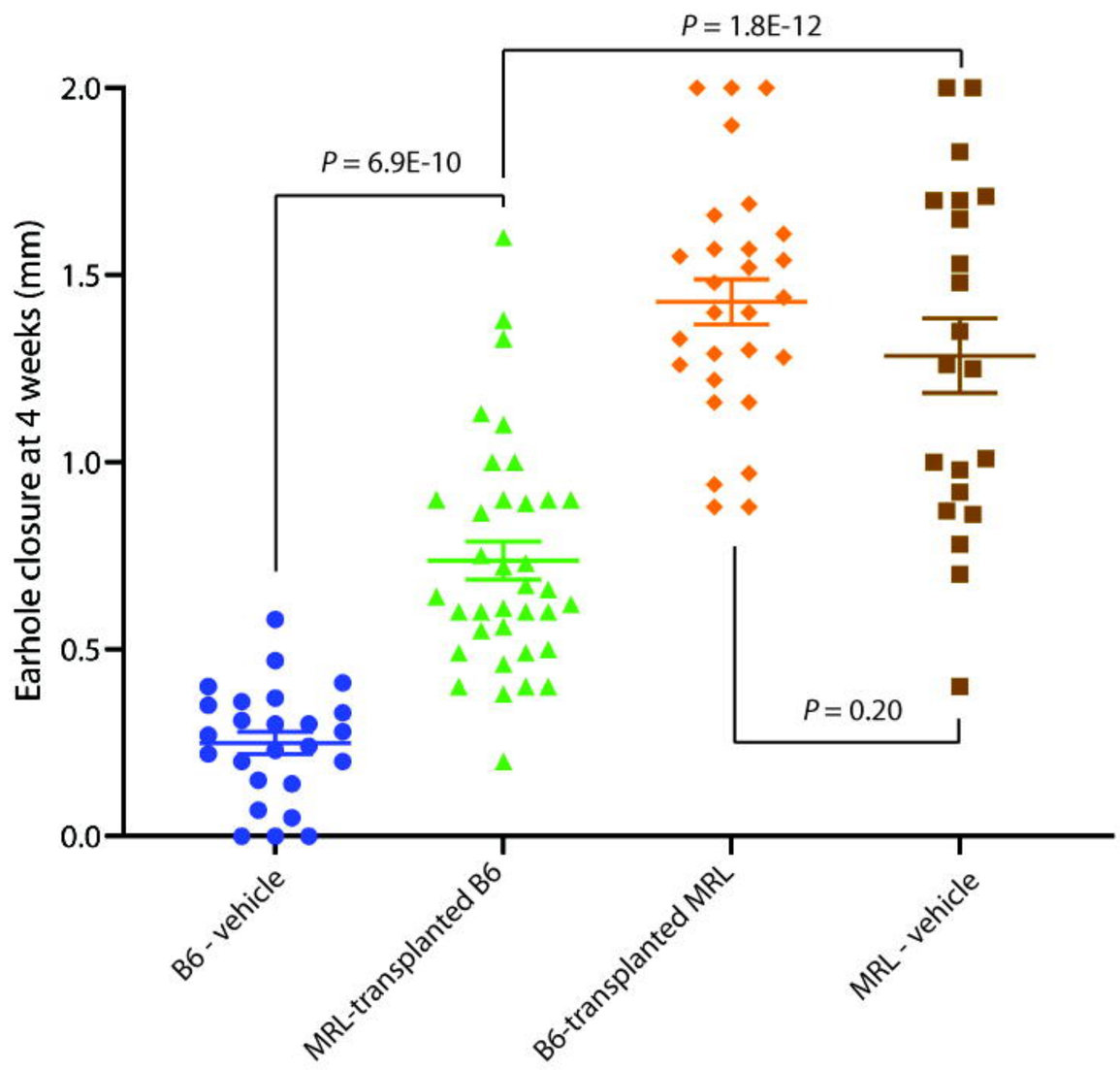

D. Earhole closure differences in mice raised in-house vs. purchased from a commercial vendor, mice transplanted at weaning

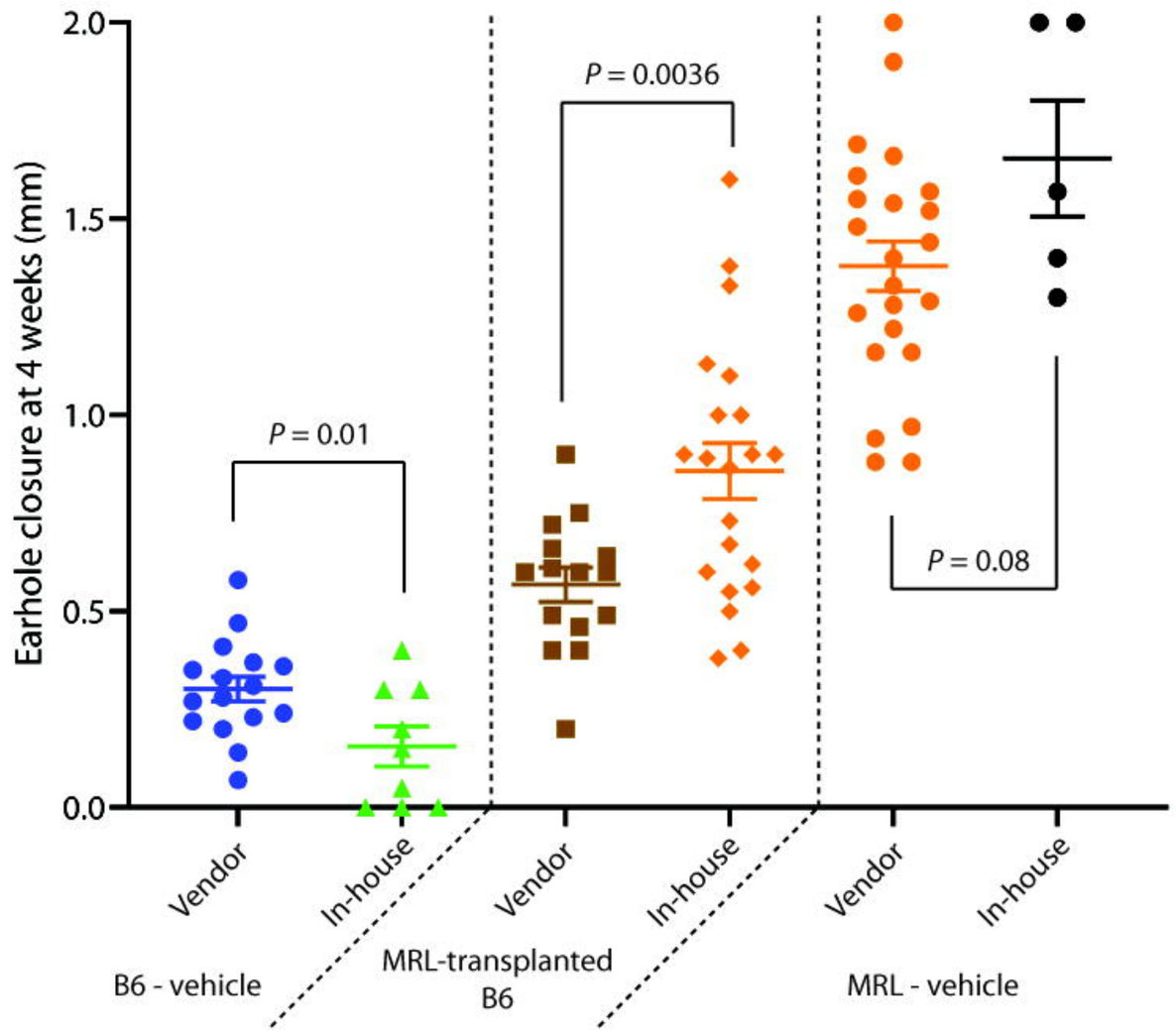

B. Earhole closure results, MRL-transplanted B6 and B6-vehicle, mice transplanted before and after ear punch

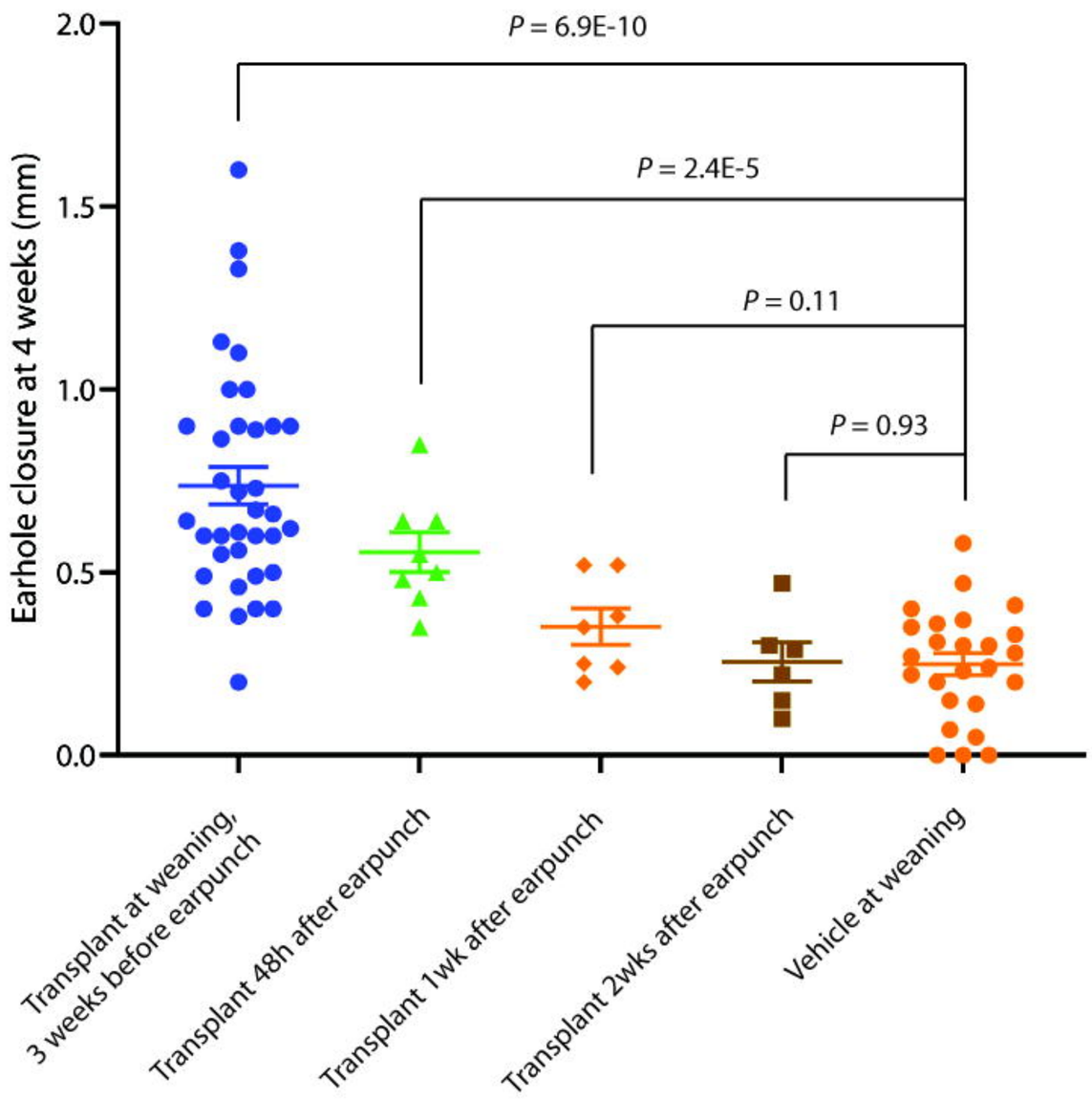

E. Earhole closure results, offspring of MRL-transplanted B6 mice

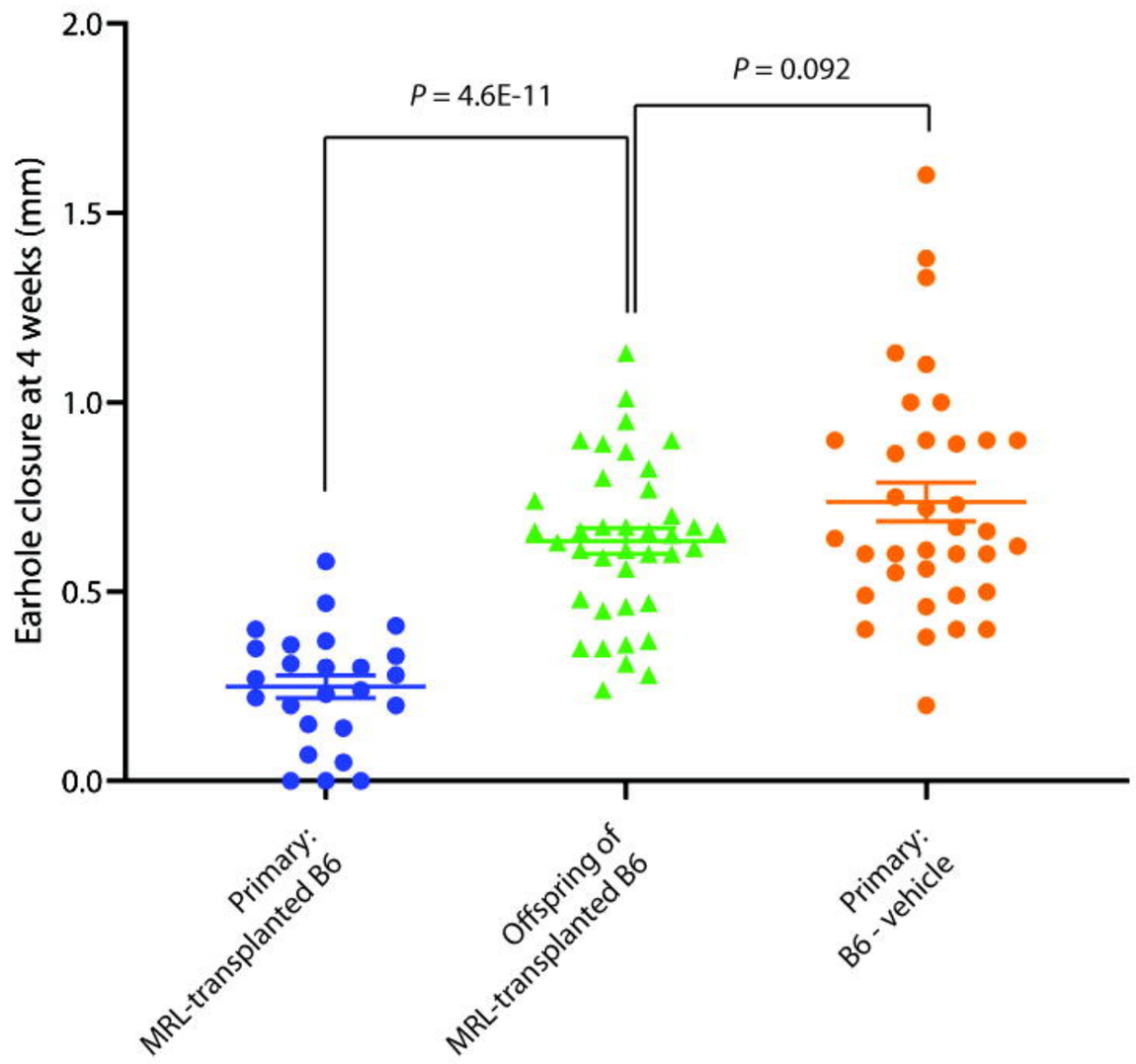

C. Earhole closure results, mice transplanated at weaning vs. as an adult (12-week)

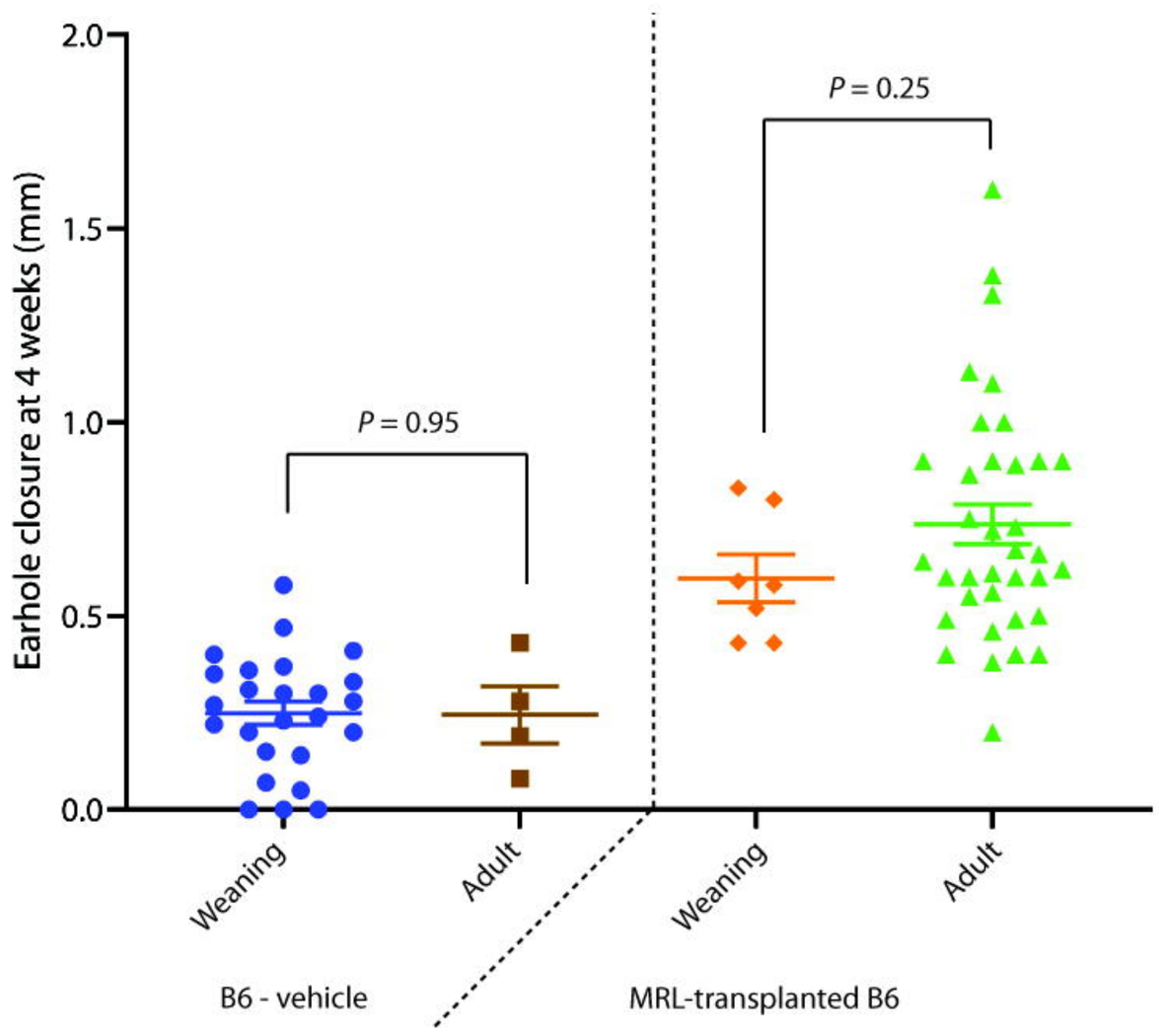

Figure 2: 16S cecal microbiome analysis

A. Alpha diversity, mouse transplant groups, by observed OTU method

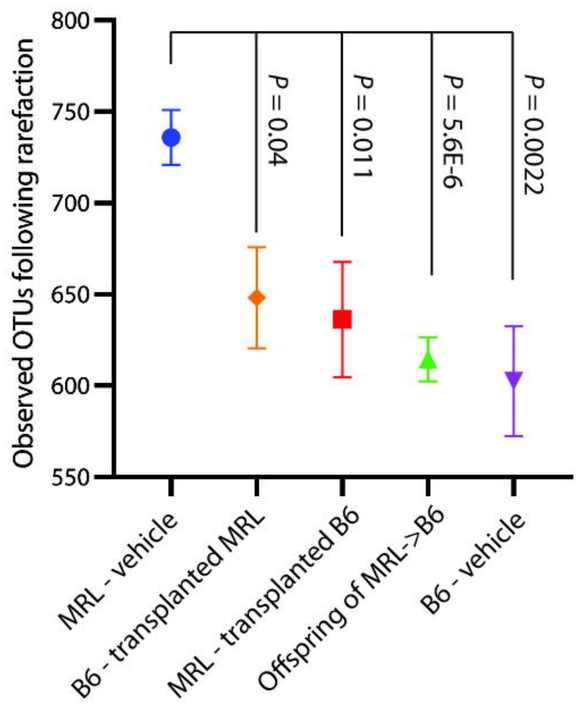

B. Beta diversity, mouse transplant groups, by weighted unifrac method

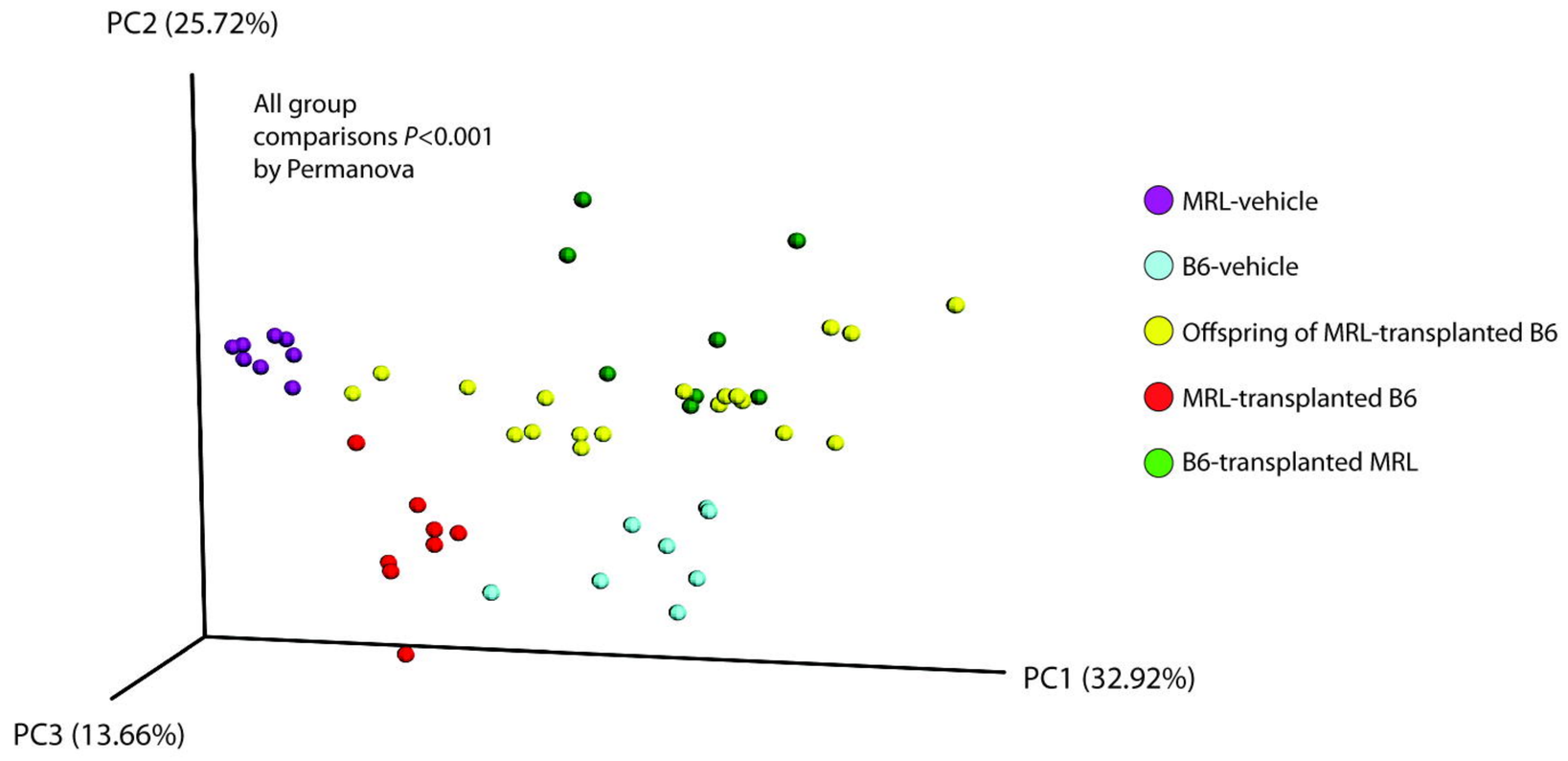

C. Cecal microbiome differences by transplant group

MRL-vehicle vs. B6-vehicle

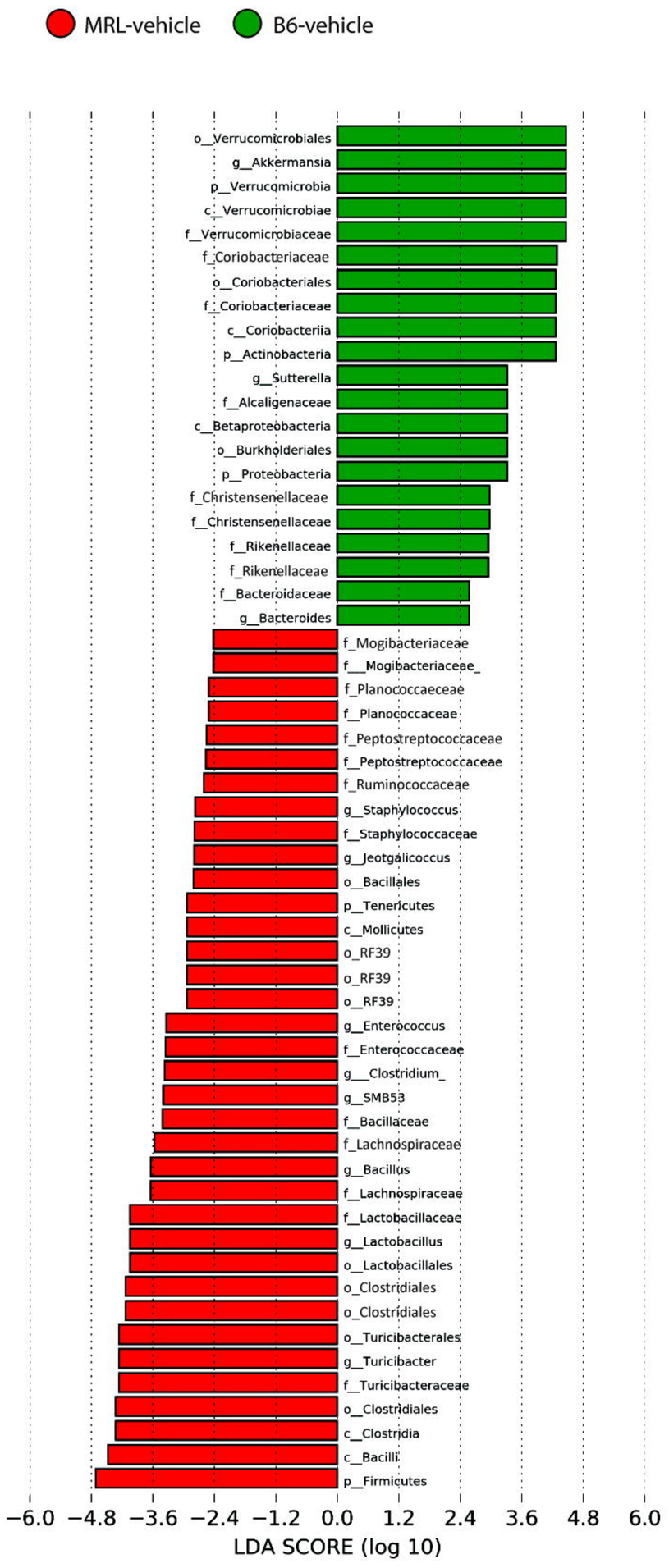

MRL-transplanted B6 vs. B6-vehicle

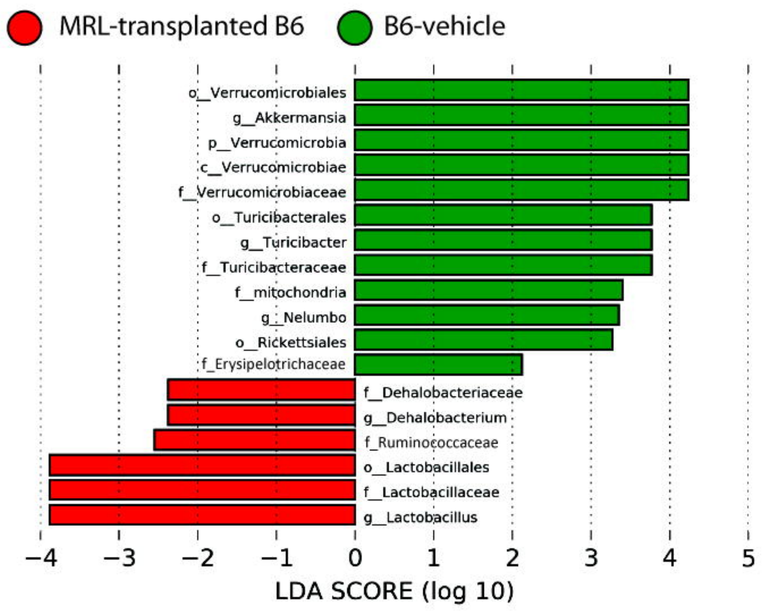

Progeny of MRL-transplanted B6 vs. B6-vehicle

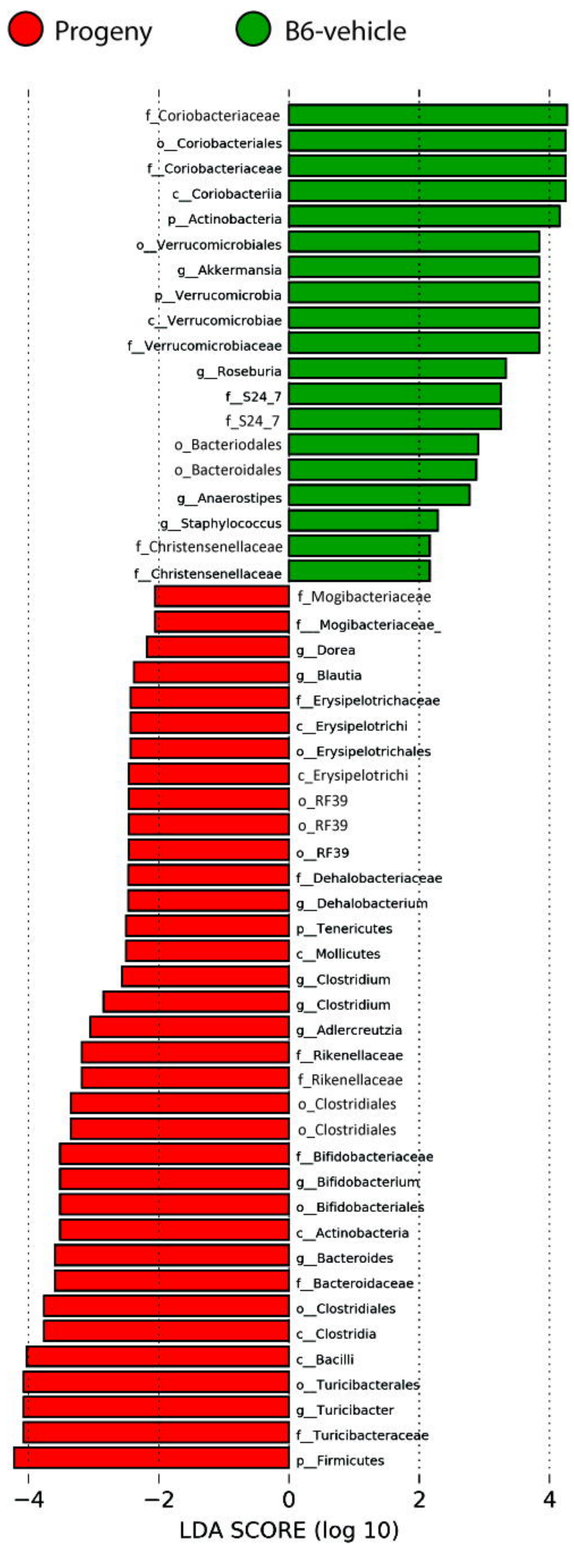

B6-transplanted MRL vs. MRL-vehicle

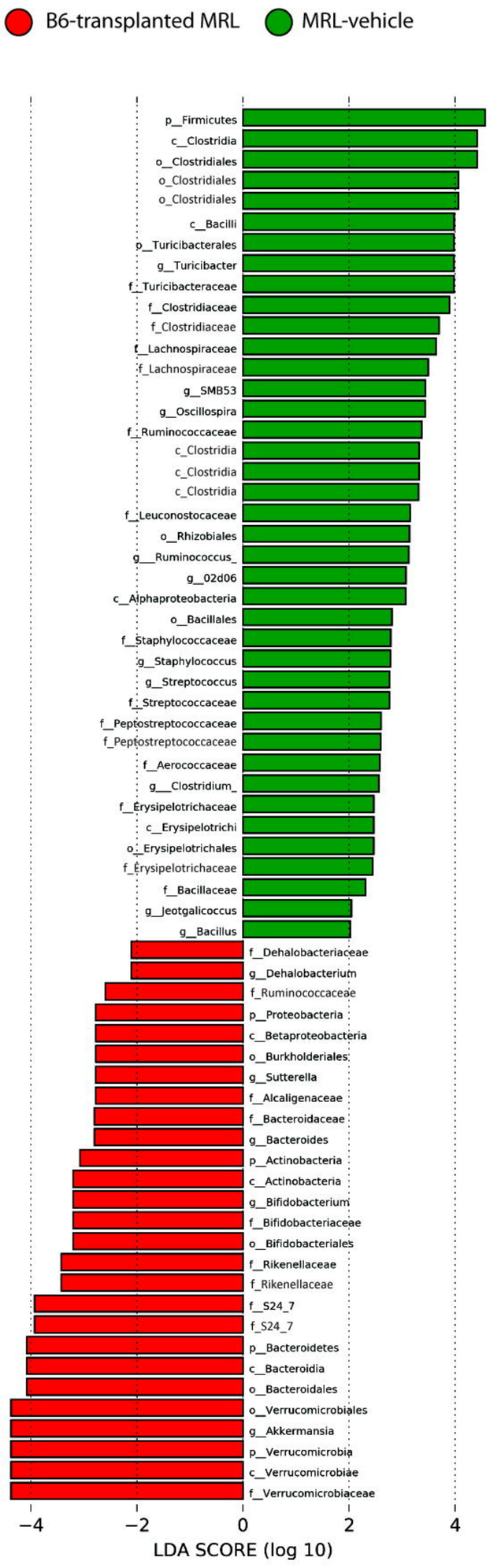

D. Specific cecal clades correlated with earhole closure rates in MRL-vehicle, B6-vehicle, MRL-transplanted B6, and progeny of MRL-transplanted B6 mice

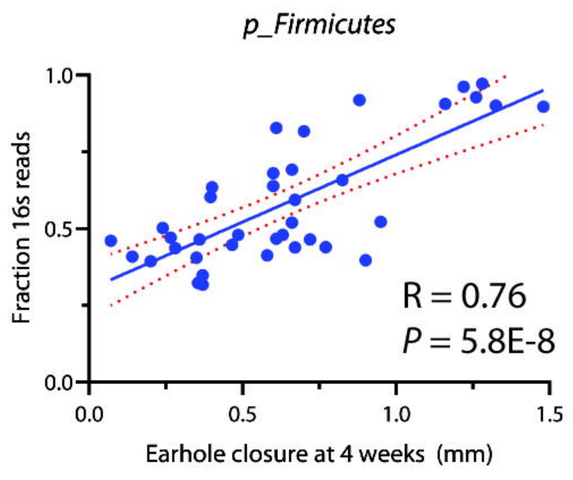

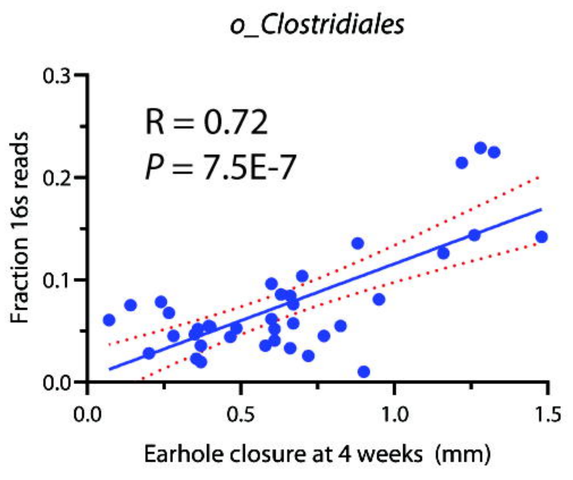

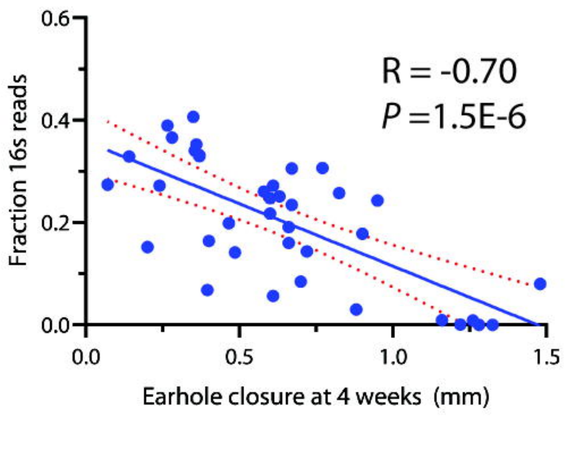

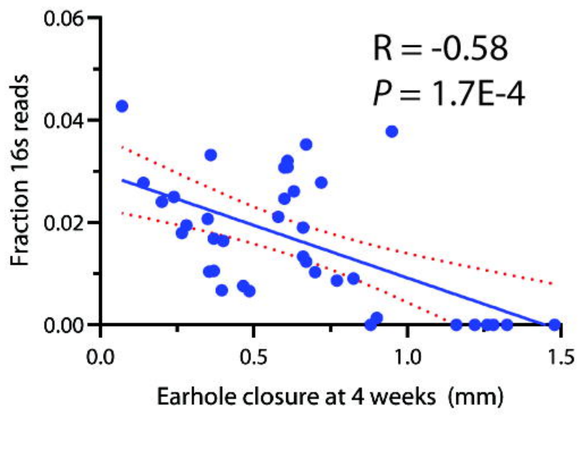

E. Cecal microbiome Gram negative proportions

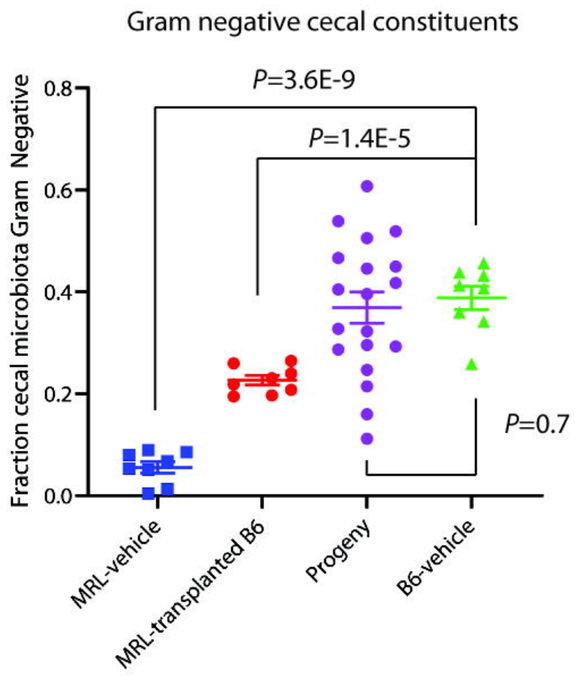

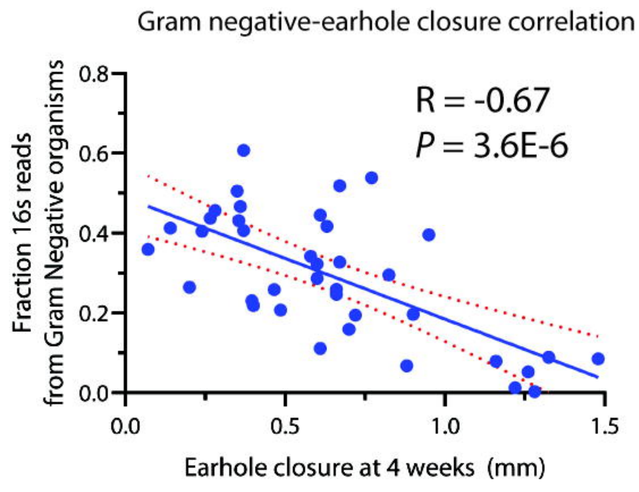

Figure 3: Mouse earhole closure and cecal microbiome analysis 4 weeks after 2.0mm ear punch, separated by mouse sex

A. Earhole closure results, segregated by mouse sex, mice transplanted at weaning

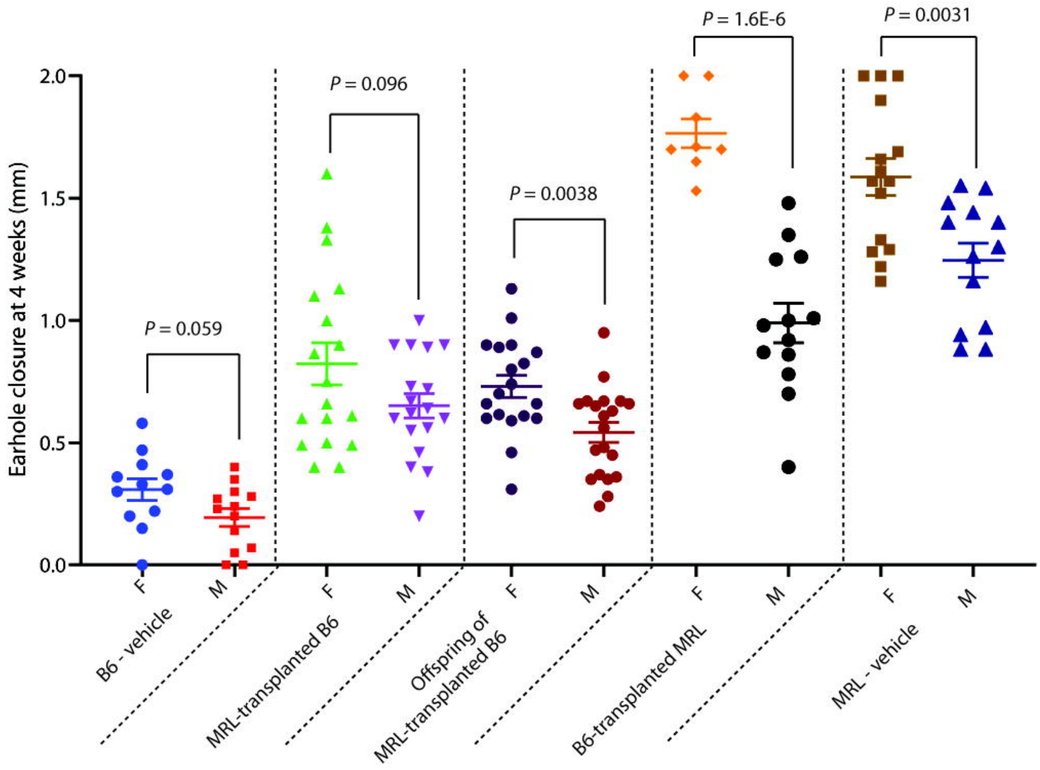

B. Beta diversity, mouse sex, by weighted unifrac method. Mouse transplant groups within dotted ellipses.

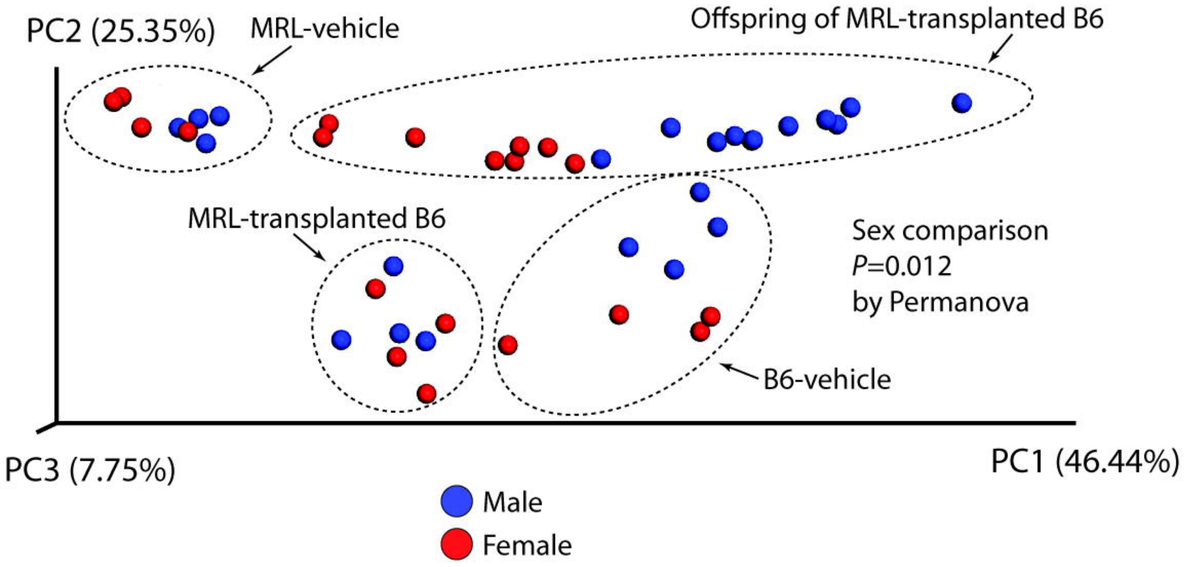
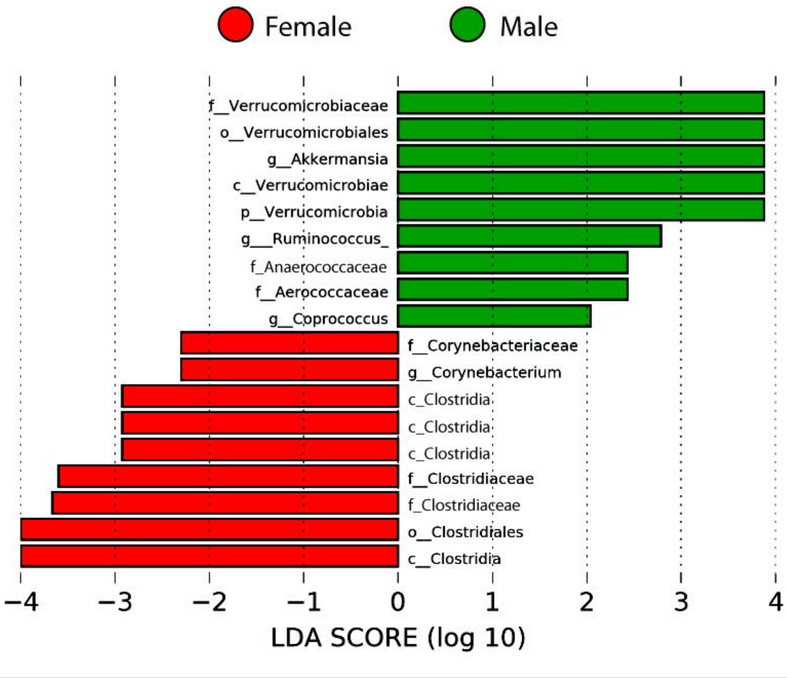
C. Cecal microbiome differences by mouse sex